Sub-50-fs Formation of Charge Transfer States Rules the Fate of Photoexcitations in Eumelanin-Like Materials

Vasilis Petropoulos[a], Alexandra Mavridi Printezi[b], Arianna Menichetti[b], Dario Mordini [b], Piotr Kabacinski[a], Nathan C. Gianneschi[c], Marco Montalti[b], Margherita Maiuri[a]*, Giulio Cerullo[a]**

[a]Dipartimento di Fisica, Politecnico di Milano, Piazza Leonardo da Vinci 32, Milano, Italy.

[b]Department of Chemistry "Giacomo Ciamician", University of Bologna, Via Selmi 2, Bologna 40126, Italy.

[c]Department of Chemistry, Northwestern University, Evanston, Illinois 60208, USA.

AUTHOR INFORMATION

Corresponding Author

* marco.montalti2@unibo.it, margherita.maiuri@polimi.it, giulio.cerullo@polimi.it

Abstract

Eumelanins play a crucial role as photoprotective agents for living organisms, yet the nature of the stationary and transient species involved in the light absorption and deactivation processes remains

controversial. Moreover, the critical sub-100-fs timescale, which is key to the characterization of the primary excited species, has remained unexplored. Here we study the eumelanin analogue polydopamine (PDA) and employ a combination of steady-state and transient optical spectroscopy techniques to reveal the presence of spectrally broad coupled electronic transitions with, at least partial, charge-transfer (CT) character. We monitor the CT state dynamics using tunable sub-20-fs pulses. We find that high photon energy excitation results in accelerated (sub-20-fs) CT formation rates, while activating pathways which lead to long-lived (>> 1 ns), possibly reactive CT species. On the other hand, visible light excitation results in a slower (≈45-fs) formation of bound CT states, which however recombine on the ultrafast sub-2-ps timescale.

TOC GRAPHICS

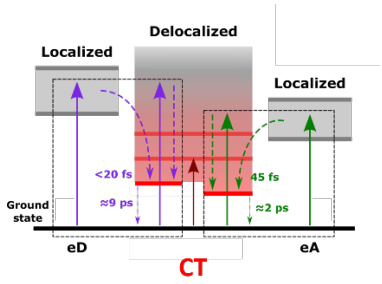

Light absorption in biomimetic melanin nanoparticles involves both localized and delocalized excited states. Charge transfer interactions play a major role in determining the broad absorption spectrum typical of eumelanin-like nanomaterials.

KEYWORDS Polydopamine, Melanin, Photoprotection, Ultrafast transient absorption, Charge transfer states.

Main text

Melanins constitute a family of multifunctional bio-pigments with diverse structures and origins that protect living species by displaying a variety of defense mechanisms.[1–3] Mammalian eumelanin, in particular, plays a key role as photo-protection agent.[4] Despite its fundamental importance, the structure and chemical composition of eumelanin and its analogues remain elusive, and the origin of its spectrally broad and featureless absorption spectrum is still an open question.[5,6] The models used to elucidate the optical properties of eumelanin range from considering subsets of weakly interacting chromophores[7–10] to incorporating strong excitonic[11–14] and/or charge transfer (CT)[15–17] couplings.

So far, the understanding of the nature of the transient species responsible for the ultrafast deactivation processes in eumelanin has been hindered by the limited time resolution of experimental techniques, particularly in the critical sub-100-fs range. Kohler *et al*. posited that eumelanin functions as a biopolymer, wherein photoprotectant CT states emerge at timescales possibly even faster than 100-fs.[15,18,19] In contrast, Hodgkiss *et al*.[13] suggested that neutral collective excitations (excitons) promptly localize the absorbed photon energy to lower energy species on the sub-100-fs timescale. Excited state deactivation, which takes place within mere picoseconds, is explained by the CT state recombination in the former case and by localized excitons undergoing partial excited-state proton transfer in the latter case.

Here we investigate polydopamine (PDA), the synthetic analogue of eumelanin, which has been reported to possess the same photo-protective action as natural eumelanin and to be so similar in structure that they can undergo the same biological pathways, being efficiently internalized by human keratinocytes.[1,20–22] By employing steady-state absorption and ultrafast transient absorption

(TA) spectroscopy, we provide additional support to the hypothesis that CT interactions within eumelanin's primary species can lead to broadband absorption, effectively reproducing the red-near-infrared (NIR) spectrum of PDA. Thanks to our high temporal resolution, we observe in real time the primary photophysical event of the formation of CT-states on the sub-100-fs timescale. Interestingly, we find that UV light absorption with large excess energy promotes the nearly instantaneous (sub-20-fs) formation of long-lived (>> 1 ns) CT species. In contrast, visible light absorption results in a slower (45-fs) formation time of bound CT-states, which efficiently recombine on the sub-2-ps timescale.

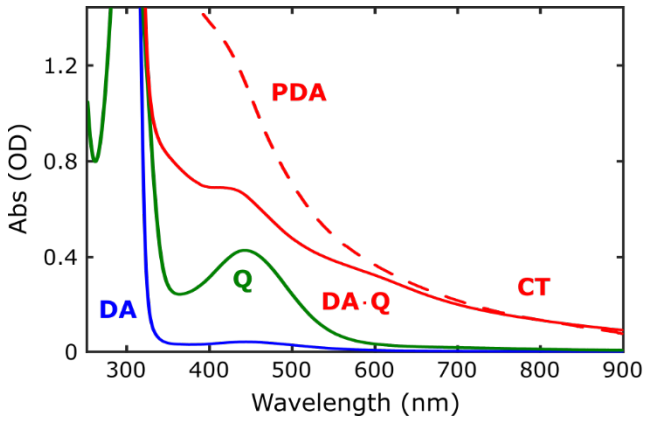

Figure 1: Absorption spectrum of DA (0.7 mM) in the absence of oxygen blue line. In the presence of atmospheric oxygen DA is oxidized to from Q (0.7 mM) to give the green line spectrum. Q solution was hence de-oxygenated and DA 7 mM was added. The absorption spectrum (continuous red line) is very different from the combination of the spectra of Q and DA revealing the formation od a DA·Q adduct with new CT band clearly detectable in the 600-900 nm region. The spectrum of the adduct is compared with the one of PDA (dashed red line).

In the limit of non-interacting chromophores, bottom-up synthetic methodologies have aimed at producing 5,6-dihydroxyindole (DHI) and/or 5,6-dihydroxyindole-2-carboxylic acid (DHICA) based oligomeric eumelanin analogues under anaerobic conditions.[23,24] However, these approaches

fall short in replicating the red-NIR absorption signatures (i.e., λ > 600 nm), highlighting the involvement of their oxidized counterparts in determining the optical properties of eumelanin-like materials.[1,25] To demonstrate that low energy absorption of PDA can be the result of CT transitions involving the PDA precursor, dopamine (DA), as electron donor (eD) moiety and its oxidized quinonic unit (Q) as electron acceptor (eA), we conducted a simple experiment.[16] We stress that indeed oxidized forms of DA are known to occur in the PDA formation, since this process involves the oxidation/polymerization of DA by environmental oxygen. As depicted in Figure 1, in an oxygen-free solution, DA remains unoxidized and absorbs only in the UV region (λ<350 nm). However, under low concentration (0.7 mM) in the presence of oxygen, the oxidized form Q is produced, with an absorption peak at approximately 460 nm. The spectrum of Q remains unchanged even after the removal of oxygen. Neither DA nor Q exhibit any significant absorption at λ > 600 nm. In contrast, when the two components are mixed in the absence of oxygen, a completely different spectrum emerges, displaying a broad absorption band that encompasses additional oscillator strengths across the UV to visible-NIR wavelength ranges (DA·Q, red solid line). This result leads to the conclusion that the ground state CT interaction between eD and eA units found in PDA is capable of generating broad absorption bands, possessing transitions in the visible/NIR region that match the absorption of PDA.

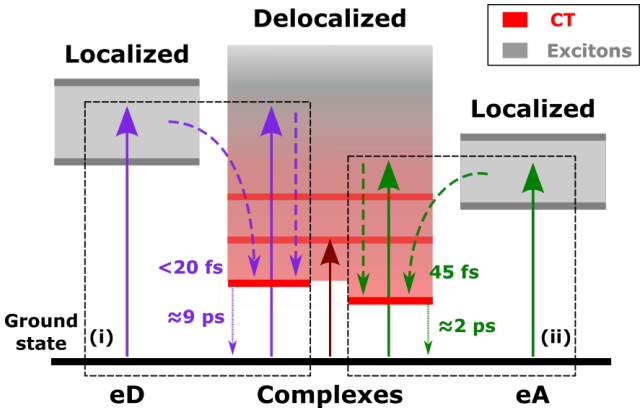

Figure 2: Simplified scheme of the electronic states and transitions involved in PDA. The eD and eA are represented by a ladder of states stemming from PDAs chemical disorder. The coupled complexes result in substantial CT character (red) while excitonically coupled or uncoupled chromophores result in neutral excitonic contributions (grey). The overall couplings enhance the absorption oscillator strengths from UV to NIR regions. Highlighted in boxes are the deactivation channels following (i) UV and (ii) visible excitations respectively.

Considering the well-known chemical heterogeneity of eumelanin-like materials,[10,11,18] we can extend our dimeric model's energy level scheme (Figure S3 in the Supporting Information (SI)) to incorporate different donor-acceptor species with substantial CT couplings. As shown in Figure 2, in practice the energy levels of DA and Q are replaced by a ladder of states stemming from the different donor and acceptor species respectively. Nevertheless, it is crucial to acknowledge that the copresence of uncoupled and excitonically coupled chromophores cannot be ruled out, resulting in excited states characterized by localized and delocalized excitons, respectively.

In light of our proposed energy level scheme, we aim to examine the dominant excited state species in PDA and their deactivation mechanisms using tunable 100-fs excitation pulses. Excitation of PDA at 266 nm results in a broad and structureless excited state absorption (ESA) spanning from the visible to the NIR , peaking at 650 nm, and reaching its maximum amplitude within our temporal resolution (Figures 3a,b). Closely matching ESA responses have been reported for other eumelanin-like materials.[13,18,26,27] Visible excitation at 500 nm yields a similar ESA response, with a slightly red-shifted peak at 700 nm due to the competing ground state bleaching (GSB) signal that decreases ESA's amplitude at the spectral region close to the pump wavelength (Figures 3d,e). This GSB signal appears as a hole burned around the excitation wavelength in the TA spectrum and is attributed to eumelanin's chemical disorder (Figures S7 and S8).[11,18]

Throughout our 1-ns pump-probe delay window, the spectral shape of the ESA signal remains unchanged, indicating the absence of intermediates after its sub-100 fs formation (Figures 3a,d and Figures S4-S8). However, the main deactivation channel seems to be favored under visible ($<\tau>\approx 2$ ps; process shown as a faded dotted green arrow in Figure 2ii) excitation compared to UV ($<\tau>\approx 9$ ps; process shown as a faded dotted violet arrow in Figure 2i).

If the ESA signature originated solely from the population of optically bright neutral excitonic species, it would be challenging to explain the absence of radiative decay in such long-lived residual excitonic transitions,[19] as testified by the extremely low (< 0.1%) fluorescence quantum yields of eumelanin's excited state[28,29]. Cascaded excitation energy transfer (EET) pathways[7,8] or internal conversion to intermediate dark states[13] on picosecond timescales, involving lower energy species with similar spectroscopic ESA signatures, could explain the lack of fluorescence. However, such processes should lead to changes in the transition dipole moment of the excited state, manifesting as an ultrafast depolarization of the ESA signal.[30,31] The absence of such a depolarization, indicated by the time-independent TA anisotropy dynamics (Figures 3c,f), speaks against such excitonic quenching mechanisms.

Thus, the most plausible explanation is that the ESA signal arises from dark states forming on sub-100-fs timescales. Low energy neutral excitonic dark states could emerge from dipole-dipole interactions within aggregates.[32] However, this configuration has a tendency to enhance the absorption oscillator strength at high photon energies, and has proven ineffective to experimentally account for the broad vis-NIR absorption tail observed in eumelanin-like materials.[24] Alternatively, the mixing between Frenkel excitons and CT states might yield red-shifted absorption bands with pronounced CT character.[32,33] This phenomenon could effectively reproduce the broadband absorption spectrum of PDA, as we demonstrated earlier in this paper. Importantly, the broad and

featureless ESA band suggests the presence of bound CT species,[34] aligning with the observed low fluorescence quantum yields.[35] Taken together, these findings strongly indicate that photoprotective CT states, forming on sub-100 fs timescales, are the dominant excited state species of eumelanin-like materials.

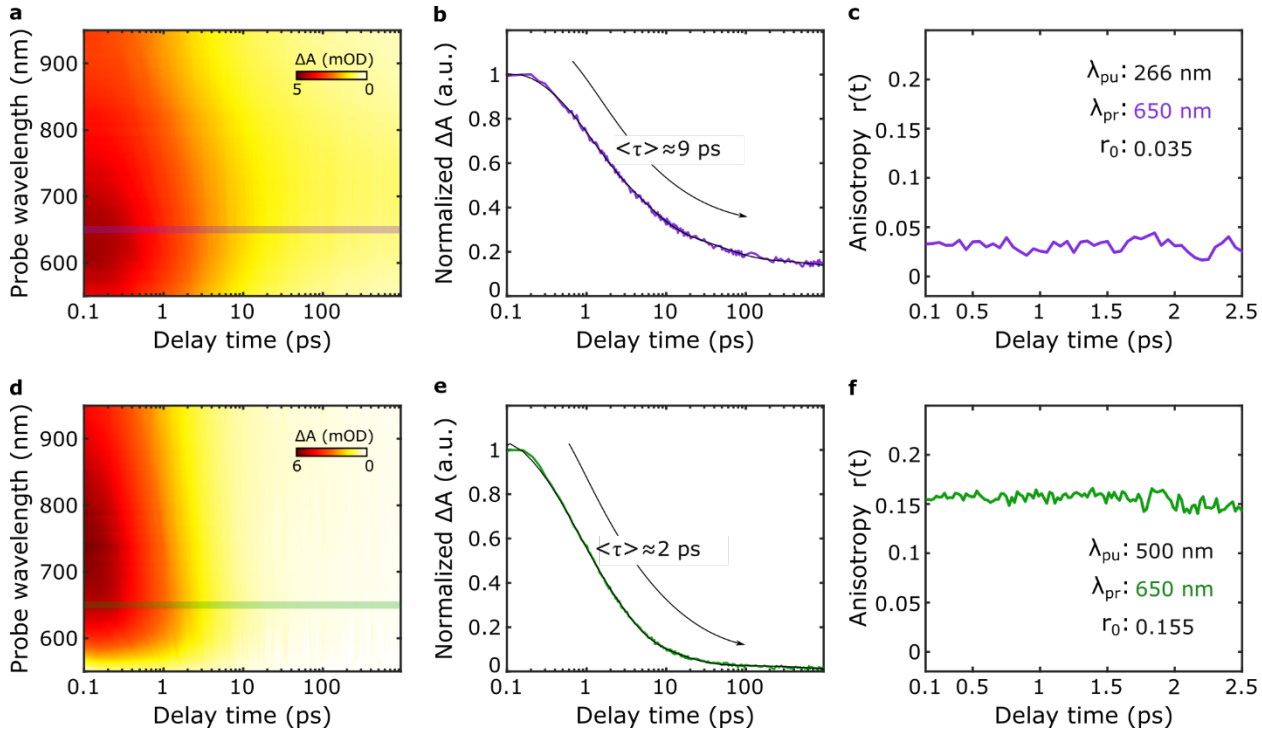

Figure 3: **(a, d)** TA maps of PDA, as a function of wavelength and time, **(b, e)** kinetic traces and **(c, f)** anisotropy dynamics at 650 nm detection wavelength obtained upon **(a, b, c)** 266 nm and **(d, e, f)** 500 nm excitation, using sub-100-fs pulses.

To uncover the sub-100-fs excited state dynamics of PDA, we carried out ultrafast TA experiments using sub-20-fs excitation pulses centered at 285 nm (Figure 4a) and 520 nm (Figure 4e), respectively, while detecting the response at visible wavelengths. Figures 4b and 4f show the dynamics of the ESA signals probed at 645 nm under both UV and visible excitations, respectively,

superimposed with their corresponding fits extracted by global analysis (Figures S10-S13).[36] Notably, pumping at 520 nm results in a time-resolved formation of the ESA signal attributed to CT states, occurring with a time constant of ≈40 fs. To eliminate the possibility of overlapping GSB signal, possibly produced by our broadband excitation with spectrum spanning 500-670 nm (see the 'Materials and Methods' section in SI), affecting the ESA dynamics at 645 nm, we took the additional step of adjusting our probe window to the 860-1000 nm range in the NIR (Figure 4c), where any possible contribution of GSB becomes negligible. Interestingly, the ESA signal is observed to rise with a similar ≈45-fs time constant for longer probed wavelengths (Figure 4d; process shown as dashed green non-radiative transitions in Figure 2ii). Conversely, upon UV excitation at 285 nm, the ESA signal of the CT states forms instantaneously within the instrumental response function (IRF) of the system (process shown as dashed violet lines in Figure 2i). This finding suggests the presence of additional ultrafast CT formation channels activated upon UV excitation in contrast to visible light absorption, as previously suggested by Kohler *et al*.[19].

According to the recently proposed excitonic model of eumelanin,[13] sub-100 fs cascaded internal conversion to lower energy species should manifest as a dynamic red-shift of the forming GSB and ESA bands in ultrafast TA experiments. However, our experimental findings present a contrasting behavior, with a broad ESA band spanning 550-1000 nm, peaking around the 660 nm, that builds up synchronously with a 40-45 fs time constant upon visible excitation and does not display any further spectral evolution. On a similar timescale, the observation of an isosbestic point at 531 nm (Figure 4e and Figure S14), that aligns with the delayed formation of an excited state population characterized by broad ESA band, indicates a dynamic equilibrium between the CT and ground state populations (see the section 'Isosbestic point in transient absorption signals' in SI). Neutral excitons and CT states might be formed concurrently after light absorption, however

our experimental data strongly indicate that the nature of the excited state shifts towards the CT character on the sub-50-fs timescale.

Recently, the formation of CT states between oxidized and reduced indolic units of eumelanin on the sub-100-fs timescale has been suggested.[15,37] The formation of CT-states in PDA takes place on the ≈40-fs timescale upon visible excitation and becomes faster than our IRF under UV excitation. Such formation of photoprotective CT-states is one order of magnitude faster with respect to the previously assigned creation of zwitterionic forms in non-interacting oligomeric analogues of eumelanin,[24] highlighting the importance of the CT couplings on the excited state pathways.

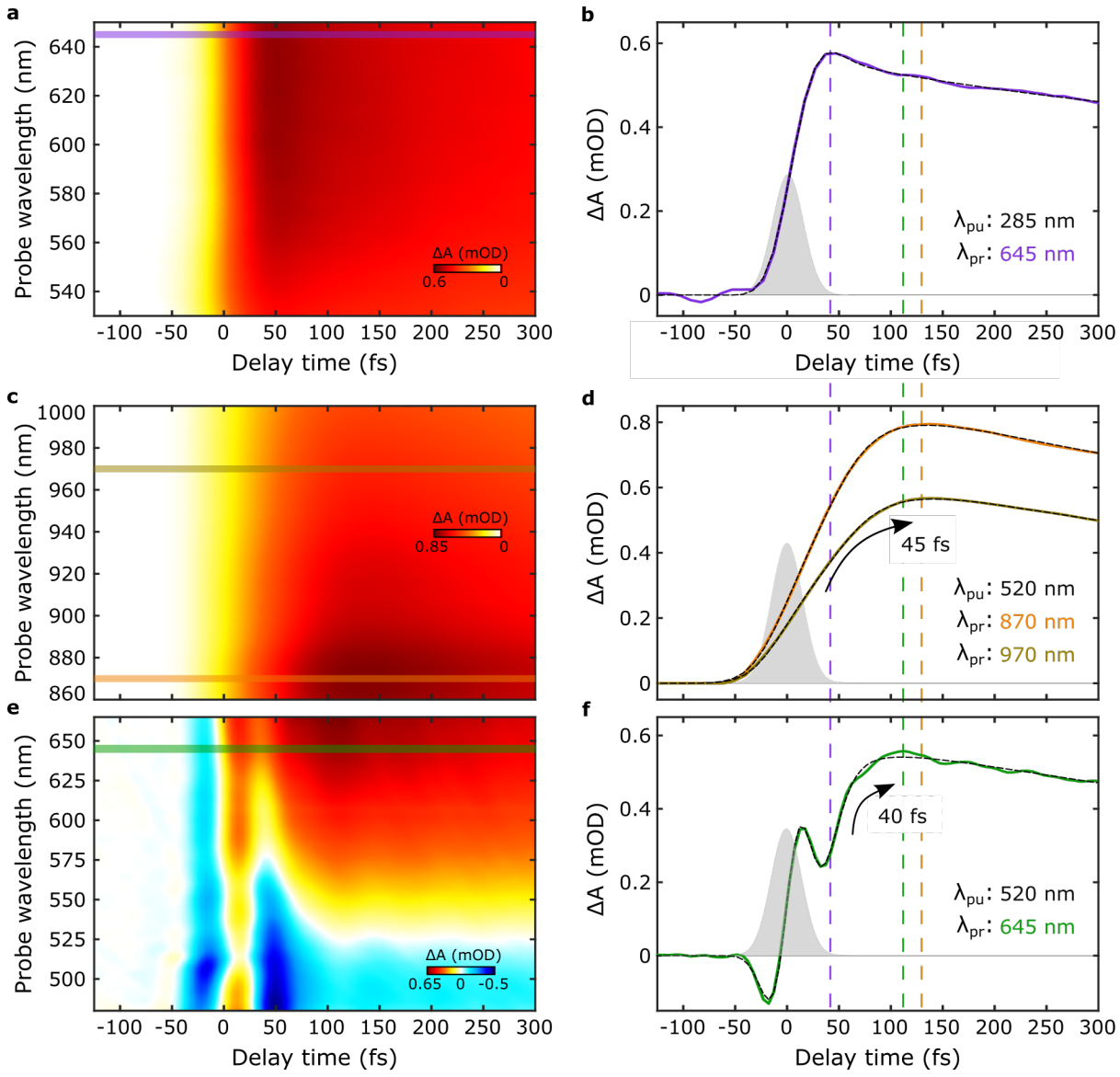

Figure 4: Formation dynamics of the CT-states. **(a, c, e)** TA maps as a function of wavelength and time upon excitation **(a)** at 285 nm and **(c, e)** at 520 nm. The colored rectangles show the chosen probed wavelength at 645 nm for **(a, e)** and at 870 nm, 970 nm for **(c)**, used for monitoring the formation of the CT-states respectively. **(b, d, f)** Tracking the ESA kinetics stemming from the CT-states following excitation **(b)** at 285 nm and **(d, f)** at 520 nm, superimposed with their fits (black dotted line) extracted by global analysis. The grey Gaussian represents our IRF (sub-30 fs).

When tuning the pump from the UV to the visible, a faster CT recombination dynamics on the sub-10-ps timescale accompanied by a lower amplitude of the long-lived CT population residuals (> 1 ns) was observed (Figure 3b,e; Figure S9 and Tables S2,S3). UV excitation results in faster formation of the CT states but with subsequent slower recombination times compared to visible excitation. From a quantitative perspective, the ratio of the CT formation rate over the charge recombination rate provides a better estimation of the long-lived character of the CT states.[38] Importantly, we observed a 10-fold increase in this ratio upon UV excitation compared to visible excitation, indicating the presence of a long-lived CT population, which can be associated with the higher photo-reactivity of melanins under high photon energy excitation.[39,40] Our data strengthen observations of excitation wavelength-dependent responses in emission[28,29], free radical production[41], and heat dissipation[42] in both natural and synthetic eumelanins.

In conclusion, our work addresses the ongoing controversy surrounding the identification of ground and excited state species in eumelanin-like materials. We support the hypothesis that eumelanin acts as a biopolymer and find that CT states can explain the broadband and structureless absorption spectrum, while serving as the predominant excited state deactivation channel on sub-50-fs timescales. Upon UV excitation, the system acquires a large excess energy, enabling excitons to explore numerous decay channels into closely lying CT states, thereby increasing the rate of CT state formation (<20-fs time constant).[19,43] Consequently, high photon energies can activate channels of separated charges, explaining the presence of long-lived CT species (>> 1 ns).[44] On the other hand, visible excitation provides less excess energy, creating localized bound charges that may be trapped by energetic barriers.[43] This leads to a slower (45-fs time constant) formation of CT states but to faster (sub-2-ps) recombination dynamics, promoting the ultrafast deactivation of the excited state. Our findings represent a significant advance in the understanding of the

chromophoric interactions and excited state decay pathways of eumelanin, and of the photoprotection mechanism at play when they are subjected to tunable photoexcitation ranging from UV to NIR.

ASSOCIATED CONTENT

(Word Style "TE_Supporting_Information"). **Supporting Information**. A listing of the contents.

The following files are available free of charge.

brief description (file type, i.e., PDF)

brief description (file type, i.e., PDF)

AUTHOR INFORMATION

Notes

The authors declare no competing financial interests.

ACKNOWLEDGMENT

This project has received funding from the European Union's Horizon 2020 research and innovation programme under the Marie Sklodowska-Curie grant No 812992 ("MUSIQ" network).

REFERENCES

(1) Cao, W.; Zhou, X.; McCallum, N. C.; Hu, Z.; Ni, Q. Z.; Kapoor, U.; Heil, C. M.; Cay, K. S.; Zand, T.; Mantanona, A. J.; Jayaraman, A.; Dhinojwala, A.; Deheyn, D. D.; Shawkey, M. D.; Burkart, M. D.; Rinehart, J. D.; Gianneschi, N. C. Unraveling the Structure and Function of Melanin through Synthesis. *J Am Chem Soc* **2021**, *143* (7), 2622–2637. https://doi.org/10.1021/jacs.0c12322.

(2) Huang, L.; Liu, M.; Huang, H.; Wen, Y.; Zhang, X.; Wei, Y. Recent Advances and Progress on Melanin-like Materials and Their Biomedical Applications. *Biomacromolecules* **2018**, *19* (6), 1858–1868. https://doi.org/10.1021/acs.biomac.8b00437.

(3) Koike, S.; Yamasaki, K. Melanogenesis Connection with Innate Immunity and Toll-Like Receptors. *Int J Mol Sci* **2020**, *21* (24), 9769. https://doi.org/10.3390/ijms21249769.

(4) d'Ischia, M.; Wakamatsu, K.; Cicoira, F.; Di Mauro, E.; Garcia-Borron, J. C.; Commo, S.; Galván, I.; Ghanem, G.; Kenzo, K.; Meredith, P.; Pezzella, A.; Santato, C.; Sarna, T.; Simon, J. D.; Zecca, L.; Zucca, F. A.; Napolitano, A.; Ito, S. Melanins and Melanogenesis: From Pigment Cells to Human Health and Technological Applications. *Pigment Cell Melanoma Res* **2015**, *28* (5), 520–544. https://doi.org/10.1111/pcmr.12393.

(5) Pralea, I.-E.; Moldovan, R.-C.; Petrache, A.-M.; Ilieș, M.; Hegheș, S.-C.; Ielciu, I.; Nicoară, R.; Moldovan, M.; Ene, M.; Radu, M.; Uifălean, A.; Iuga, C.-A. From Extraction to Advanced Analytical Methods: The Challenges of Melanin Analysis. *Int J Mol Sci* **2019**, *20* (16), 3943. https://doi.org/10.3390/ijms20163943.

(6) Mavridi-Printezi, A.; Menichetti, A.; Guernelli, M.; Montalti, M. The Photophysics and Photochemistry of Melanin- Like Nanomaterials Depend on Morphology and Structure. *Chemistry – A European Journal* **2021**, *27* (66), 16309–16319. https://doi.org/10.1002/chem.202102479.

(7) Forest, S. E.; Lam, W. C.; Millar, D. P.; Nofsinger, J. B.; Simon, J. D. A Model for the Activated Energy Transfer within Eumelanin Aggregates. *J Phys Chem B* **2000**, *104* (4), 811–814. https://doi.org/10.1021/jp992137l.

(8) Meredith, P.; Powell, B. J.; Riesz, J.; Nighswander-Rempel, S. P.; Pederson, M. R.; Moore, E. G. Towards Structure–Property–Function Relationships for Eumelanin. *Soft Matter* **2006**, *2* (1), 37–44. https://doi.org/10.1039/B511922G.

(9) Tran, M. L.; Powell, B. J.; Meredith, P. Chemical and Structural Disorder in Eumelanins: A Possible Explanation for Broadband Absorbance. *Biophys J* **2006**, *90* (3), 743–752. https://doi.org/10.1529/biophysj.105.069096.

(10) d'Ischia, M.; Napolitano, A.; Pezzella, A.; Meredith, P.; Sarna, T. Chemical and Structural Diversity in Eumelanins: Unexplored Bio-Optoelectronic Materials. *Angewandte Chemie International Edition* **2009**, *48* (22), 3914–3921. https://doi.org/10.1002/anie.200803786.

(11) Thompson, A.; Robles, F. E.; Wilson, J. W.; Deb, S.; Calderbank, R.; Warren, W. S. Dual-Wavelength Pump-Probe Microscopy Analysis of Melanin Composition. *Sci Rep* **2016**, *6* (1), 36871. https://doi.org/10.1038/srep36871.

(12) Chen, C.-T.; Chuang, C.; Cao, J.; Ball, V.; Ruch, D.; Buehler, M. J. Excitonic Effects from Geometric Order and Disorder Explain Broadband Optical Absorption in Eumelanin. *Nat Commun* **2014**, *5* (1), 3859. https://doi.org/10.1038/ncomms4859.

(13) Ilina, A.; Thorn, K. E.; Hume, P. A.; Wagner, I.; Tamming, R. R.; Sutton, J. J.; Gordon, K. C.; Andreassend, S. K.; Chen, K.; Hodgkiss, J. M. The Photoprotection Mechanism in the

Black–Brown Pigment Eumelanin. *Proceedings of the National Academy of Sciences* **2022**, *119* (43). https://doi.org/10.1073/pnas.2212343119.

(14) Ju, K.-Y.; Fischer, M. C.; Warren, W. S. Understanding the Role of Aggregation in the Broad Absorption Bands of Eumelanin. *ACS Nano* **2018**, *12* (12), 12050–12061. https://doi.org/10.1021/acsnano.8b04905.

(15) Grieco, C.; Kohl, F. R.; Hanes, A. T.; Kohler, B. Probing the Heterogeneous Structure of Eumelanin Using Ultrafast Vibrational Fingerprinting. *Nat Commun* **2020**, *11* (1), 4569. https://doi.org/10.1038/s41467-020-18393-w.

(16) Mavridi-Printezi, A.; Menichetti, A.; Ferrazzano, L.; Montalti, M. Reversible Supramolecular Noncovalent Self-Assembly Determines the Optical Properties and the Formation of Melanin-like Nanoparticles. *J Phys Chem Lett* **2022**, *13* (42), 9829–9833. https://doi.org/10.1021/acs.jpclett.2c02239.

(17) Choudhury, A.; Ghosh, D. Charge Transfer in DHICA Eumelanin-like Oligomers: Role of Hydrogen Bonds. *Chemical Communications* **2020**, *56* (72), 10481–10484. https://doi.org/10.1039/D0CC04702C.

(18) Kohl, F. R.; Grieco, C.; Kohler, B. Ultrafast Spectral Hole Burning Reveals the Distinct Chromophores in Eumelanin and Their Common Photoresponse. *Chem Sci* **2020**, *11* (5), 1248–1259. https://doi.org/10.1039/C9SC04527A.

(19) Grieco, C.; Kohl, F. R.; Kohler, B. Ultrafast Radical Photogeneration Pathways in Eumelanin †. *Photochem Photobiol* **2023**, *99* (2), 680–692. https://doi.org/10.1111/php.13731.

(20) Huang, Y.; Li, Y.; Hu, Z.; Yue, X.; Proetto, M. T.; Jones, Y.; Gianneschi, N. C. Mimicking Melanosomes: Polydopamine Nanoparticles as Artificial Microparasols. *ACS Cent Sci* **2017**, *3* (6), 564–569. https://doi.org/10.1021/acscentsci.6b00230.

(21) Cao, W.; McCallum, N. C.; Ni, Q. Z.; Li, W.; Boyce, H.; Mao, H.; Zhou, X.; Sun, H.; Thompson, M. P.; Battistella, C.; Wasielewski, M. R.; Dhinojwala, A.; Shawkey, M. D.; Burkart, M. D.; Wang, Z.; Gianneschi, N. C. Selenomelanin: An Abiotic Selenium Analogue of Pheomelanin. *J Am Chem Soc* **2020**, *142* (29), 12802–12810. https://doi.org/10.1021/jacs.0c05573.

(22) Zhou, X.; McCallum, N. C.; Hu, Z.; Cao, W.; Gnanasekaran, K.; Feng, Y.; Stoddart, J. F.; Wang, Z.; Gianneschi, N. C. Artificial Allomelanin Nanoparticles. *ACS Nano* **2019**, *13* (10), 10980–10990. https://doi.org/10.1021/acsnano.9b02160.

(23) D'Ischia, M.; Crescenzi, O.; Pezzella, A.; Arzillo, M.; Panzella, L.; Napolitano, A.; Barone, V. Structural Effects on the Electronic Absorption Properties of 5,6-Dihydroxyindole Oligomers: The Potential of an Integrated Experimental and DFT Approach to Model Eumelanin Optical Properties †. *Photochem Photobiol* **2008**, *84* (3), 600–607. https://doi.org/10.1111/j.1751-1097.2007.00249.x.

(24) Corani, A.; Huijser, A.; Gustavsson, T.; Markovitsi, D.; Malmqvist, P.-Å.; Pezzella, A.; d'Ischia, M.; Sundström, V. Superior Photoprotective Motifs and Mechanisms in Eumelanins Uncovered. *J Am Chem Soc* **2014**, *136* (33), 11626–11635. https://doi.org/10.1021/ja501499q.

(25) Micillo, R.; Panzella, L.; Iacomino, M.; Prampolini, G.; Cacelli, I.; Ferretti, A.; Crescenzi, O.; Koike, K.; Napolitano, A.; d'Ischia, M. Eumelanin Broadband Absorption Develops from Aggregation-Modulated Chromophore Interactions under Structural and Redox Control. *Sci Rep* **2017**, *7* (1), 41532. https://doi.org/10.1038/srep41532.

(26) Brunetti, A.; Arciuli, M.; Triggiani, L.; Sallustio, F.; Gallone, A.; Tommasi, R. Do Thermal Treatments Influence the Ultrafast Opto-Thermal Processes of Eumelanin? *European Biophysics Journal* **2019**, *48* (2), 153–160. https://doi.org/10.1007/s00249-018-1342-y.

(27) Ye, T.; Simon, J. D. Comparison of the Ultrafast Absorption Dynamics of Eumelanin and Pheomelanin. *J Phys Chem B* **2003**, *107* (40), 11240–11244. https://doi.org/10.1021/jp0352837.

(28) Meredith, P.; Riesz, J. Radiative Relaxation Quantum Yields for Synthetic Eumelanin ¶. *Photochem Photobiol* **2004**, *79* (2), 211–216. https://doi.org/10.1111/j.1751-1097.2004.tb00012.x.

(29) Nighswander-Rempel, S. P.; Riesz, J.; Gilmore, J.; Meredith, P. A Quantum Yield Map for Synthetic Eumelanin. *J Chem Phys* **2005**, *123* (19). https://doi.org/10.1063/1.2075147.

(30) Kang, S.; Kaufmann, C.; Hong, Y.; Kim, W.; Nowak-Król, A.; Würthner, F.; Kim, D. Ultrafast Coherent Exciton Dynamics in Size-Controlled Perylene Bisimide Aggregates. *Structural Dynamics* **2019**, *6* (6). https://doi.org/10.1063/1.5124148.

(31) Hamerlynck, L. M.; Bischoff, A. J.; Rogers, J. R.; Roberts, T. D.; Dai, J.; Geissler, P. L.; Francis, M. B.; Ginsberg, N. S. Static Disorder Has Dynamic Impact on Energy Transport in Biomimetic Light-Harvesting Complexes. *J Phys Chem B* **2022**, *126* (40), 7981–7991. https://doi.org/10.1021/acs.jpcb.2c06614.

(32) Hestand, N. J.; Spano, F. C. Expanded Theory of H- and J-Molecular Aggregates: The Effects of Vibronic Coupling and Intermolecular Charge Transfer. *Chem Rev* **2018**, *118* (15), 7069–7163. https://doi.org/10.1021/acs.chemrev.7b00581.

(33) Kim, J. H.; Schembri, T.; Bialas, D.; Stolte, M.; Würthner, F. Slip-Stacked J-Aggregate Materials for Organic Solar Cells and Photodetectors. *Advanced Materials* **2022**, *34* (22). https://doi.org/10.1002/adma.202104678.

(34) Etzold, F.; Howard, I. A.; Mauer, R.; Meister, M.; Kim, T.-D.; Lee, K.-S.; Baek, N. S.; Laquai, F. Ultrafast Exciton Dissociation Followed by Nongeminate Charge Recombination in PCDTBT:PCBM Photovoltaic Blends. *J Am Chem Soc* **2011**, *133* (24), 9469–9479. https://doi.org/10.1021/ja201837e.

(35) Hu, Z.; Willard, A. P.; Ono, R. J.; Bielawski, C. W.; Rossky, P. J.; Vanden Bout, D. A. An Insight into Non-Emissive Excited States in Conjugated Polymers. *Nat Commun* **2015**, *6* (1), 8246. https://doi.org/10.1038/ncomms9246.

(36) Snellenburg, J. J.; Laptenok, S. P.; Seger, R.; Mullen, K. M.; Stokkum, I. H. M. van. **Glotaran** : A *Java* -Based Graphical User Interface for the *R* Package **TIMP**. *J Stat Softw* **2012**, *49* (3). https://doi.org/10.18637/jss.v049.i03.

(37) Matta, M.; Pezzella, A.; Troisi, A. Relation between Local Structure, Electric Dipole, and Charge Carrier Dynamics in DHICA Melanin: A Model for Biocompatible Semiconductors. *J Phys Chem Lett* **2020**, *11* (3), 1045–1051. https://doi.org/10.1021/acs.jpclett.9b03696.

(38) Hou, Y.; Zhang, X.; Chen, K.; Liu, D.; Wang, Z.; Liu, Q.; Zhao, J.; Barbon, A. Charge Separation, Charge Recombination, Long-Lived Charge Transfer State Formation and Intersystem Crossing in Organic Electron Donor/Acceptor Dyads. *J Mater Chem C Mater* **2019**, *7* (39), 12048–12074. https://doi.org/10.1039/C9TC04285G.

(39) Mostert, A. B.; Rienecker, S. B.; Noble, C.; Hanson, G. R.; Meredith, P. The Photoreactive Free Radical in Eumelanin. *Sci Adv* **2018**, *4* (3). https://doi.org/10.1126/sciadv.aaq1293.

(40) Solano, F. Photoprotection *versus* Photodamage: Updating an Old but Still Unsolved Controversy about Melanin. *Polym Int* **2016**, *65* (11), 1276–1287. https://doi.org/10.1002/pi.5117.

(41) Sarna, T.; Sealy, R. C. Free Radicals from Eumelanins: Quantum Yields and Wavelength Dependence. *Arch Biochem Biophys* **1984**, *232* (2), 574–578. https://doi.org/10.1016/0003-9861(84)90575-7.

(42) S. E. Forest, J. D. Simon, Wavelength-dependent Photoacoustic Calorimetry Study of Melanin. Photochem. Photobiol. **1998**, 68, 296–298.

(43) Grancini, G.; Maiuri, M.; Fazzi, D.; Petrozza, A.; Egelhaaf, H.-J.; Brida, D.; Cerullo, G.; Lanzani, G. Hot Exciton Dissociation in Polymer Solar Cells. *Nat Mater* **2013**, *12* (1), 29–33. https://doi.org/10.1038/nmat3502.

(44) Bakulin, A. A.; Rao, A.; Pavelyev, V. G.; van Loosdrecht, P. H. M.; Pshenichnikov, M. S.; Niedzialek, D.; Cornil, J.; Beljonne, D.; Friend, R. H. The Role of Driving Energy and Delocalized States for Charge Separation in Organic Semiconductors. *Science (1979)* **2012**, *335* (6074), 1340–1344. https://doi.org/10.1126/science.1217745.